UC San Diego
UC San Diego Previously Published Works

Title

Human species-specific loss of CMP-*N*-acetylneuraminic acid hydroxylase enhances atherosclerosis via intrinsic and extrinsic mechanisms.

Permalink

https://escholarship.org/uc/item/15c2w48d

Journal

Proceedings of the National Academy of Sciences of the United States of America, 116(32)

ISSN

0027-8424

Authors

Kawanishi, Kunio
Dhar, Chirag
Do, Raymond
et al.

Publication Date

2019-08-01

DOI

10.1073/pnas.1902902116

Peer reviewed

Human species-specific loss of CMP-*N*-acetylneuraminic acid hydroxylase enhances atherosclerosis via intrinsic and extrinsic mechanisms

Kunio Kawanishi[a,b,1], Chirag Dhar[a,b], Raymond Do[a,c], Nissi Varki[a,c], Philip L. S. M. Gordts[a,2], and Ajit Varki[a,b,d,e,2]

[a]Glycobiology Research and Training Center, University of California San Diego, La Jolla, CA 92093; [b]Department of Cellular & Molecular Medicine, University of California San Diego, La Jolla, CA 92093; [c]Department of Pathology, University of California San Diego, La Jolla, CA 92093; [d]Department of Medicine, University of California San Diego, La Jolla, CA 92093; and [e]Center for Academic Research and Training in Anthropogeny, University of California San Diego, La Jolla, CA 92093

Cardiovascular disease (CVD) events due to atherosclerosis cause one-third of worldwide deaths and risk factors include physical inactivity, age, dyslipidemia, hypertension, diabetes, obesity, smoking, and red meat consumption. However, ~15% of first-time events occur without such factors. In contrast, coronary events are extremely rare even in closely related chimpanzees in captivity, despite human-like CVD–risk-prone blood lipid profiles, hypertension, and mild atherosclerosis. Similarly, red meat-associated enhancement of CVD event risk does not seem to occur in other carnivorous mammals. Thus, heightened CVD risk may be intrinsic to humans, and genetic changes during our evolution need consideration. Humans exhibit a species-specific deficiency of the sialic acid *N*-glycolylneuraminic acid (Neu5Gc), due to pseudogenization of cytidine monophosphate-*N*-acetylneuraminic acid (Neu5Ac) hydroxylase (*CMAH*), which occurred in hominin ancestors ~2 to 3 Mya. $Ldlr^{-/-}$ mice with human-like *Cmah* deficiency fed a sialic acids (Sias)-free high-fat diet (HFD) showed ~1.9-fold increased atherogenesis over *Cmah* wild-type $Ldlr^{-/-}$ mice, associated with elevated macrophage cytokine expression and enhanced hyperglycemia. Human consumption of Neu5Gc (from red meat) acts as a "xeno-autoantigen" via metabolic incorporation into endogenous glycoconjugates, as interactions with circulating anti-Neu5Gc "xeno-autoantibodies" potentiate chronic inflammation ("xenosialitis"). $Cmah^{-/-}Ldlr^{-/-}$ mice immunized with Neu5Gc-bearing antigens to generate human-like anti-Neu5Gc antibodies suffered a ~2.4-fold increased atherosclerosis on a Neu5Gc-rich HFD, compared with Neu5Ac-rich or Sias-free HFD. Lesions in Neu5Gc-immunized and Neu5Gc-rich HFD-fed $Cmah^{-/-}Ldlr^{-/-}$ mice were more advanced but unexplained by lipoprotein or glucose changes. Human evolutionary loss of CMAH likely contributes to atherosclerosis predisposition via multiple intrinsic and extrinsic mechanisms, and future studies could consider this more human-like model.

human evolution | atherosclerosis | *N*-glycolylneuraminic acid (Neu5Gc) | CMAH | cytidine-5′-monophosphate (CMP)-*N*-acetylneuraminic acid (Neu5Ac) hydroxylase (CMAH)

Atherosclerosis is the predominant cause of cardiovascular disease (CVD) events such as coronary thrombosis, myocardial infarction, and strokes, which are very common in humans and responsible for about one-third of deaths worldwide (1). Interestingly, these events rarely occur spontaneously in other mammals, in the absence of experimental or dietary manipulation. Human susceptibility is assumed to be due to a combination of physical inactivity and increased risk factors, such as dyslipidemia, hypertension, diabetes, obesity, red meat consumption, and smoking. However, ~15% of initial CVD events occur in humans without obvious known risk factors (2, 3). Closely related chimpanzees also have many risk factors in captivity, including hypertension (4), high low-density lipoprotein (LDL) cholesterol (5), elevated lipoprotein(a) levels (6), and a sedentary lifestyle, yet rarely suffer atherosclerotic CVD events (5, 7–10), but instead often develop a different cardiac disease, interstitial myocardial fibrosis (5, 9,

11). While extrinsic factors related to transition from hunter-gatherer lifestyle/diet to current sedentary Western conditions likely contribute to the human propensity (12–14); the prevalence of advanced atherosclerosis in well-preserved mummies from four diverse ancient cultures (15–17) suggests a disease that is intrinsic to human aging. Taken together, the data suggest that one must also consider mechanisms intrinsic to the biology of our species, that is, genetic changes that occurred during the evolution of the human species after the common ancestor with the chimpanzee (>7 Mya).

The first reported clear-cut difference at the genetic and molecular level between humans and chimpanzees was a species-specific deficiency of the common mammalian sialic acid *N*-glycolylneuraminic acid (Neu5Gc). This loss is a result of pseudogenization of the cytidine monophosphate (CMP)-*N*-acetylneuraminic acid (Neu5Ac) hydroxylase (CMAH) gene, which likely occurred in hominin ancestors about 2 to 3 Mya (18) and then fixed in the hominin lineage before the origin of modern humans (19). The loss of this common mammalian sialic acid is also associated with an excess of the sialic acid Neu5Ac, the precursor for Neu5Gc, in the glycocalyx of human cells. The intrinsic pathophysiological consequence of the loss of Neu5Gc has been extensively studied in human-like *Cmah*-deficient ($Cmah^{-/-}$, thus Neu5Gc-deficient) mice. These mice present with many human-like

phenotypes (20), are more susceptible to develop glucose intolerance (21), and have hyperreactive macrophages (22), T cells (23), and B cells (24).

In addition to intrinsic impacts of the loss of Neu5Gc production one also needs to consider its extrinsic impact, triggered by the dietary consumption of Neu5Gc (primarily derived from red meat) (25). Once Neu5Gc is absorbed by the gastrointestinal tract it can get metabolically incorporated into cellular glycoproteins and glycolipids following the same pathway utilized by the endogenous sialic acid Neu5Ac (26). In this way consumed exogenous Neu5Gc gets presented on the cell surface glycocalyx, where it can act as a foreign "xeno-autoantigen." The actual amounts incorporated appear to be very small but tend to be enriched at sites such as epithelium and endothelium (27) and even within atherosclerotic plaques (28). Even though the incorporated amounts may be small, most humans have circulating anti-Neu5Gc "xeno-autoantibodies" and can thus develop local chronic inflammation or "xenosialitis" at sites of Neu5Gc accumulation. We have already shown that this novel form of antibody-mediated inflammation can potentiate cancer progression in the human-like *Cmah*-null mouse model (29). Based on these and previous observations we have suggested that xenosialitis may also help explain the increased risk of cancer and CVD epidemiologically associated with human red meat consumption (30).

Notably, dietary red meat-associated enhancement of cancer and CVD risk has not been reported in other carnivorous mammals. The human-specific red meat-related increase in CVD risk can be partially explained by increased choline intake (with increased conversion to trimethylamine *N*-oxide), cholesterol, and saturated fat content in red meat (25, 31–34). The suggestion of oxidant damage due to dietary heme iron is confounded by the high heme-binding capacity of plasma hemopexin, with complexes being efficiently cleared by the liver (25, 35, 36). Regardless, none of these mechanisms fully explains the increased human propensity for atherosclerosis, nor the red meat-specific and human-specific nature of the dietary component of risk.

Here we test the hypothesis that human CMAH deficiency contributes to CVD risk via both intrinsic and extrinsic mechanisms. To experimentally address the intrinsic CVD consequences Cmah-deficient (*Cmah*$^{-/-}$) and congenic wild-type mice were bred into an *Ldlr*$^{-/-}$ background and fed a sialic acids (Sias)-free high-fat diet (HFD) to induce atherogenesis. We also probed the extrinsic CVD implications using *Cmah*$^{-/-}$*Ldlr*$^{-/-}$ mice immunized with control antigens with Neu5Ac or with Neu5Gc-bearing antigens to generate human-like levels of anti-Neu5Gc antibodies. Subsequent feeding of a Neu5Gc-rich diet allowed evaluation of the contribution of diet-induced xenosialitis on atherogenesis. Our results suggest that human evolutionary loss of CMAH markedly promotes atherosclerosis development via both intrinsic and extrinsic mechanisms and may help explain the heightened predisposition of humans to develop CVD.

Results

Increased Atherogenesis in *Cmah*$^{-/-}$*Ldlr*$^{-/-}$ Mice Fed a Sias-Free HFD.
Cmah$^{-/-}$ mice mimicking the human-like *Cmah* pseudogenization were crossed into an *Ldlr*$^{-/-}$ background to study the intrinsic impact of human *CMAH* loss on CVD susceptibility. Six-week-old male and female *Cmah*$^{-/-}$*Ldlr*$^{-/-}$ mice did not have noticeable phenotypic differences from *Cmah*$^{+/+}$*Ldlr*$^{-/-}$ mice and were subsequently challenged with a soy-based high-fat/high-cholesterol diet (HFD) for 12 wk to induce atherogenesis (Fig. 1*A*). Importantly, the baseline HFD is devoid of Sias (non-Sias) to avoid any influence of Neu5Gc or Neu5Ac feeding on lesion development. To assess the impact of the mutation we analyzed atherosclerosis development in male and female *Cmah*$^{-/-}$*Ldlr*$^{-/-}$ and *Cmah*$^{+/+}$*Ldlr*$^{-/-}$ mice on the Sias-free HFD. Atherosclerosis *en face* analysis demonstrated a significant 1.45-fold (in male), and 1.88-fold (in female) increase in the overall plaque area in the

aortas of *Cmah*$^{-/-}$*Ldlr*$^{-/-}$ mice (Fig. 1 *B* and *C*). The HFD regime did not induce differences in body weight gain (*SI Appendix*, Fig. S1 *A* and *B*) or organs weight (*SI Appendix*, Fig. S1 *C* and *D*). Furthermore, the diet did not induce significant differences in plasma cholesterol and triglyceride levels (*SI Appendix*, Fig. S1 *E–H*) or in lipoprotein distribution (Fig. 1 *D–G*) between *Cmah*$^{-/-}$*Ldlr*$^{-/-}$ and *Cmah*$^{+/+}$*Ldlr*$^{-/-}$ mice in either sex. To measure the impact of lesion volume and lesion composition we performed atherosclerotic lesion analysis in the aortic sinus (Fig. 2 *A* and *B*, from female mice). *Cmah*$^{-/-}$*Ldlr*$^{-/-}$ female mice have a significant 1.93-fold increase in atherosclerotic lesion volume (Fig. 2*C*). However, lesion collagen content did not change between *Cmah*$^{-/-}$*Ldlr*$^{-/-}$ and *Cmah*$^{+/+}$*Ldlr*$^{-/-}$ female mice (Fig. 2 *D* and *E*). Moreover, macrophage content in atheromas measured by F4/80 and CD68 staining was significantly reduced in *Cmah*$^{-/-}$*Ldlr*$^{-/-}$ female mice (Fig. 2 *F–I*). On the other hand, lesions from *Cmah*$^{-/-}$*Ldlr*$^{-/-}$ female mice were much more advanced, as illustrated by a 1.97-fold increase in necrotic core area in comparison with equal size lesions from *Cmah*$^{+/+}$*Ldlr*$^{-/-}$ female mice (Fig. 2 *J* and *K*). To detect earlier apoptotic events among cells and within atheroma lesions, 8-wk HFD-fed female samples were analyzed using terminal dUTP nick-end labeling (TUNEL). *Cmah*$^{-/-}$*Ldlr*$^{-/-}$ female mice showed increased TUNEL-positive cells compared to *Cmah*$^{+/+}$*Ldlr*$^{-/-}$ female mice in 8-wk HFD duration (Fig. 2 *L* and *M*), which corresponds with a larger necrotic core size in 12-wk-fed *Cmah*$^{-/-}$*Ldlr*$^{-/-}$ female mice. Overall, the results indicate that loss of *CMAH* in mice clearly increases the predisposition for atherosclerosis development without changes in body weight or lipid profiles. These data indicate that the human evolutionary loss of *CMAH* may have contributed to increased CVD predisposition in humans.

Cmah$^{-/-}$*Ldlr*$^{-/-}$ Mice Have Hyperglycemia Independent of HFD Feeding.
Impaired glucose homeostasis associated with diabetes is a known risk factor for CVD. Interestingly, *Cmah*$^{-/-}$*Ldlr*$^{-/-}$ male mice had significantly increased fasting plasma glucose levels, especially when given HFD (Fig. 3*A*). Circulating postprandial insulin levels are significantly lower in *Cmah*$^{-/-}$*Ldlr*$^{-/-}$ male mice (Fig. 3*B*) and can explain the increased fasting glucose levels (Fig. 3*A*). This phenotype is likely a result of the previously reported compromised pancreatic β-cell function (21). Notably, the HFD negated the differences among the groups (Fig. 3*C*), indicating increased insulin resistance in *Cmah*$^{-/-}$*Ldlr*$^{-/-}$ male mice as suggested by the elevated homeostatic model assessment for insulin resistance (HOMA-IR) index (Fig. 3*D*). In female *Cmah*$^{-/-}$*Ldlr*$^{-/-}$ mice fasting glucose did not change (Fig. 3*E*); however, fasting and postprandial insulin levels were significantly lower in *Cmah*$^{-/-}$*Ldlr*$^{-/-}$ female mice fed a soy-based control diet (Fig. 3*F*). HFD reduced circulating insulin levels in *Cmah*$^{+/+}$*Ldlr*$^{-/-}$ females to the same level as *Cmah*$^{-/-}$*Ldlr*$^{-/-}$ females (Fig. 3*G*) as well as insulin resistance (Fig. 3*H*).

Glucose tolerance testing revealed that both male and female *Cmah*$^{-/-}$*Ldlr*$^{-/-}$ mice have impaired glucose tolerance independent of the dietary regime (Fig. 3 *I–L*). This finding indicates that the impaired glucose metabolism is intrinsic to the loss of Neu5Gc production. Insulin sensitivity was measured (Fig. 3 *M–P*) and found to be greater in *Cmah*$^{-/-}$*Ldlr*$^{-/-}$ females compared with *Cmah*$^{+/+}$*Ldlr*$^{-/-}$ females fed the control diet (Fig. 3*O*). This could explain why *Cmah*$^{-/-}$*Ldlr*$^{-/-}$ female fasting glucose levels are equal to *Cmah*$^{+/+}$*Ldlr*$^{-/-}$ female despite reduced insulin production. Overall the data suggest that *Cmah*$^{-/-}$*Ldlr*$^{-/-}$ mice on a soy-based control diet have increased glucose intolerance and reduced insulin production. HFD conditions did not show differences in insulin sensitivity and plasma insulin levels between the groups, suggesting that an alteration in glucose production or absorption is responsible for the impaired glucose tolerance in *Cmah*$^{-/-}$*Ldlr*$^{-/-}$ mice.
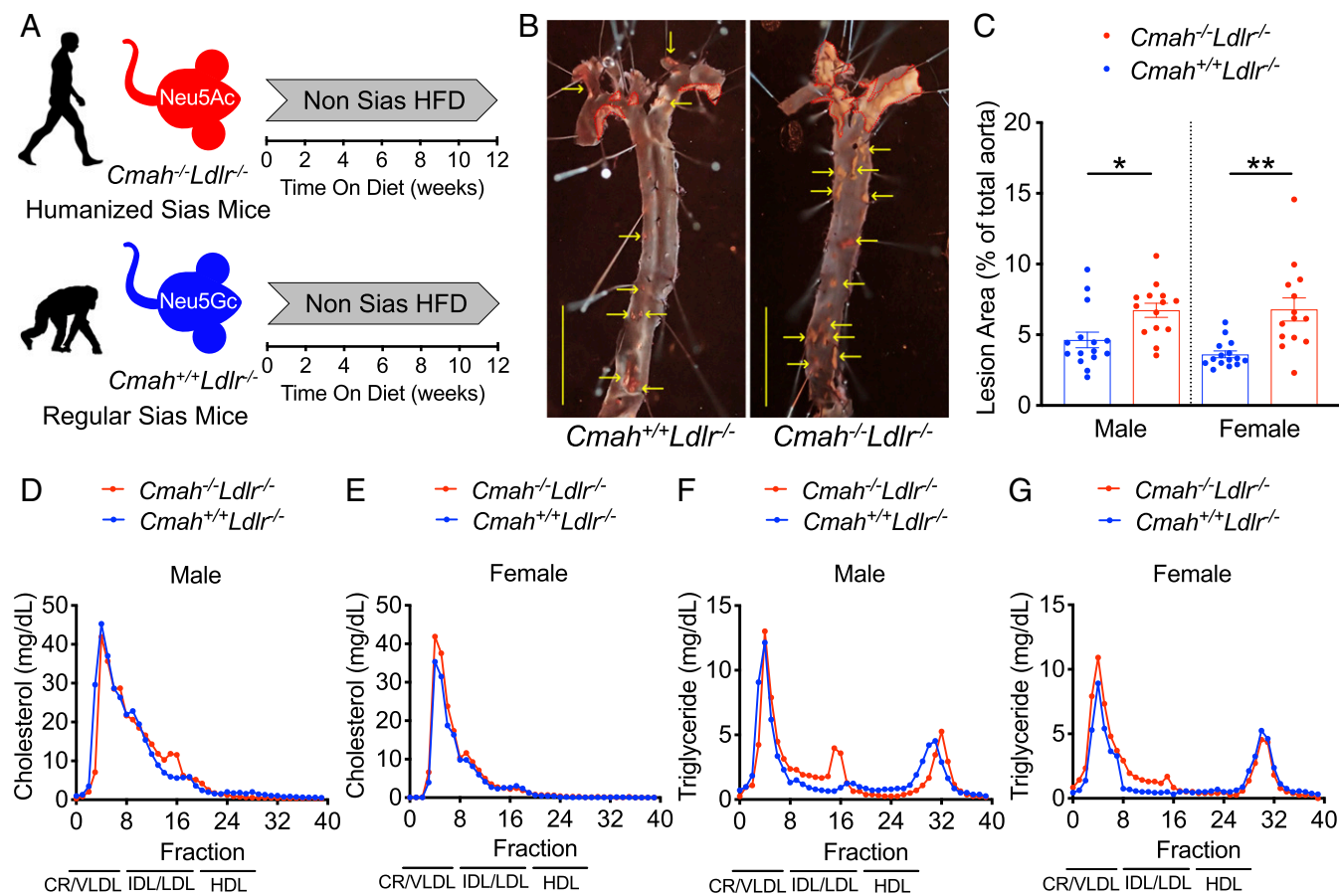
Fig. 1. $Cmah^{-/-}Ldlr^{-/-}$ increases atherogenesis without changing lipoprotein profiles. (*A*) Six-week-old $Cmah^{-/-}Ldlr^{-/-}$ and $Cmah^{+/+}Ldlr^{-/-}$ mice were put on a 12-wk soy-based non-sialic acids (Sias) high-fat diet (HFD). (*B*) *En face* analysis of atherosclerosis (red dotted areas and yellow arrows indicate atheromatous lesions in female mice) and (*C*) quantification of Sudan IV-positive area. (Scale bars, 500 μm.) (*D–G*) Fast protein liquid chromatography analysis of lipoproteins after 12 wk of HFD feeding (pooled serum from n = 14 or 15). chylomicron, CR; very-low-density lipoprotein, VLDL; intermediate density lipoprotein, IDL; low-density lipoprotein, LDL; high-density lipoprotein, HDL. Mean values ± SEM, *P < 0.05 and **P < 0.01.

Loss of *CMAH* Results in Enhanced Inflammatory Macrophages and Foam Cell Conversion. Previous studies in $Cmah^{-/-}$ mice have shown increased immune cell reactivity (22–24). This includes macrophages that present with elevated production of inflammatory cytokines and stronger phagocytic responses (22). The absence of any alterations in high-density lipoprotein (HDL) and apoB-cholesterol levels in $Cmah^{-/-}Ldlr^{-/-}$ mice suggests that a difference in the inflammatory response may explain the worsened atherosclerotic lesion development. Indeed, isolated bone marrow-derived macrophages (BMDMs) showed significantly elevated inflammatory cytokines in BMDM from $Cmah^{-/-}Ldlr^{-/-}$ female mice (Fig. 4*A*). An interesting difference between the macrophage types was the expression of ACAT1, an enzyme that converts cholesterol into cholesterol ester using long-chain fatty acyl-CoA and promotes foam cell conversion (37). We and others (37–39) previously showed that ACAT2 and ACAT1 expression is induced by inflammation in the context of hyperlipidemia. ACAT1 expression was increased in BMDMs (Fig. 4*A*) isolated from $Cmah^{-/-}Ldlr^{-/-}$ female mice. The data suggest that in the context of hyperlipidemia-induced inflammation lacking CMAH primes macrophages to express more ACAT1, thereby increasing initial foam cell conversion in vivo and not in vitro under sterile conditions.

To gain further insight into the inflammatory status of the $Cmah^{-/-}Ldlr^{-/-}$ mice, we isolated peritoneal macrophages from female mice after 12 wk on the control diet and HFD. Oil Red O staining and intracellular cholesterol ester analysis showed that the increased inflammatory status in $Cmah^{-/-}Ldlr^{-/-}$ female

macrophages was associated with >3-fold greater percentage of foam cell formation (Fig. 4 *B–D*). qPCR analysis confirmed that $Cmah^{-/-}Ldlr^{-/-}$ female mice have much more reactive peritoneal macrophages, indicated by elevated expression of many proinflammatory genes (Fig. 4 *E* and *F*). However, under sterile conditions naïve BMDMs from $Cmah^{-/-}Ldlr^{-/-}$ female mice challenged with normal human LDL, aggregated LDL (ag LDL) (40), or oxidized LDL (ox LDL) (41) did not show significantly increased foam cell conversion (*SI Appendix*, Fig. S2 *A–C*) or increased expression of inflammatory cytokines (*SI Appendix*, Fig. S2*D*). To test if alterations in local inflammatory gene expression occurred in vivo, we dissected plaques from the aortic arch and extracted mRNA for qPCR analysis, correcting transcript expression for lesion macrophage content (F4/80) in the tissue (37). Quantification of inflammatory gene expression in atherosclerotic lesions from 12-wk HFD-fed female mice confirmed a significant increase in expression of M1 macrophage-type cytokines such as *Il6* and *iNos2* (Fig. 4*G*).

We also asked if loss of CMAH affects proliferation of hematopoietic stem and pluripotent progenitor cells in the bone marrow by inducing a monocytosis that could explain the increased expression of monocyte-derived inflammatory genes in atherosclerotic lesions. However, $Cmah^{-/-}Ldlr^{-/-}$ and $Cmah^{+/+}Ldlr^{-/-}$ mice showed no difference in total white blood cell counts (*SI Appendix*, Fig. S3 *A–D*). Neutrophil counts (*SI Appendix*, Fig. S3 *E–H*) and lymphocyte counts (*SI Appendix*, Fig. S3 *I–L*) showed only minor differences at later times in each dietary
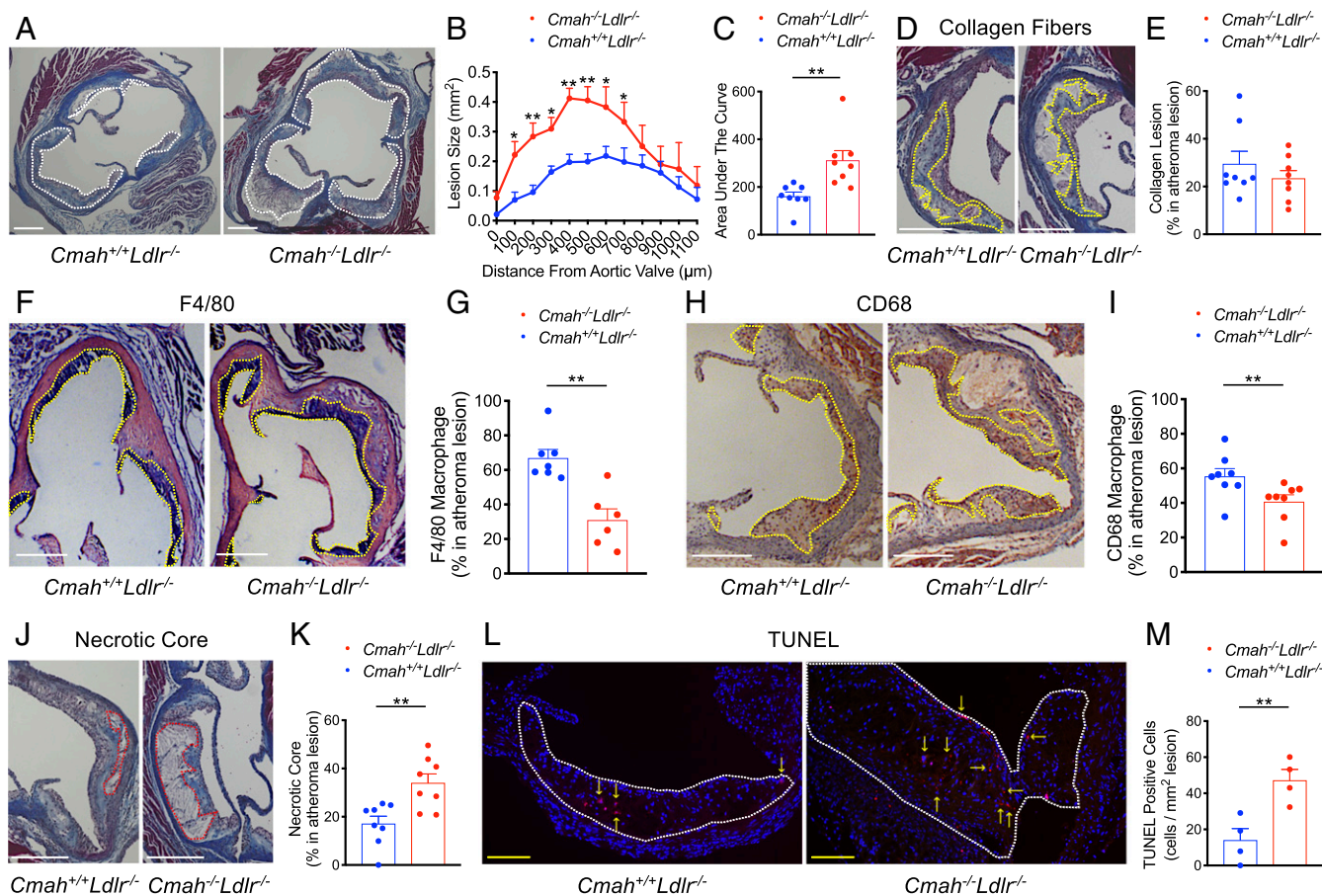
Fig. 2. $Cmah^{-/-}Ldlr^{-/-}$ increases atherogenesis without increased macrophage infiltration. Aortic sinus samples from $Cmah^{+/+}Ldlr^{-/-}$ and $Cmah^{-/-}Ldlr^{-/-}$ mice were analyzed after high-fat diet (HFD) feeding. (A and B) Quantification of total atherosclerotic lesion size (white dots) in the aortic sinus. (C) Area under the curve data. (D and E) Collagen fiber lesion (yellow dots) and analysis with Masson's trichrome stain (female, $n = 8$ each, HFD for 12 wk). (F and G) F4/80-positive lesion area (yellow dots) and analysis. (H and I) CD68-positive lesion area (yellow dots) and analysis for measuring macrophage infiltration (female, $n = 6$ to 8, HFD for 12 wk). (J and K) Necrotic core (red dots) size analysis with Masson's trichrome stain (female, $n = 8$ each, HFD for 12 wk). (L and M) Apoptotic cells (red color, yellow arrows) were detected with TUNEL per square millimeter lesion (white dots) (female, $n = 4$ each, HFD for 8 wk). (White scale bars, 300 μm; yellow scale bars, 100 μm.) Mean values ± SEM, *$P < 0.05$ and **$P < 0.01$.

group. In contrast, HFD feeding induced a significant progressive decay in the percentage of plasma monocyte counts (*SI Appendix*, Fig. S4 *A–D*). This decay was less pronounced in $Cmah^{-/-}Ldlr^{-/-}$ female mice, resulting in relatively elevated plasma monocyte counts during the HFD feeding (*SI Appendix*, Fig. S4 *C and D*), which would have contributed to the atherogenic phenotype. Interestingly, plasma monocyte counts in $Cmah^{-/-}Ldlr^{-/-}$ females was decreased to the same level as $Cmah^{+/+}Ldlr^{-/-}$ females at later times in the HFD regime (*SI Appendix*, Fig. S4D). Male $Cmah^{-/-}Ldlr^{-/-}$ mice presented with monocytosis under the control diet and not during the HFD regime (*SI Appendix*, Fig. S4 *A and B*), indicating that the increased atherosclerosis in male mice was likely not a result of monocytosis. In general, our data show that the loss of *Cmah* has sex-specific effects that overall will increase the inflammatory and atherogenic predisposition in both sexes. Additionally, the temporary monocytosis in $Cmah^{-/-}Ldlr^{-/-}$ female during the HFD feeding did not result in increased hepatic steatosis (*SI Appendix*, Fig. S4 *E–H*) and only presented a mild increased cytokine expression in the liver, pancreas, heart, and kidney (*SI Appendix*, Fig. S4 *I–L*). It suggested that the increased monocyte counts in $Cmah^{-/-}Ldlr^{-/-}$ female plasma did not result in a massive inflammatory macrophage infiltration in the organs (measured by F4/80 expression) and only modestly increased inflammation compared with $Cmah^{+/+}Ldlr^{-/-}$ females during

the HFD regime. Interestingly we did see an increased expression of the alternative macrophage marker Ym-1 in peritoneal macrophage and some tissues analyzed, suggesting increased activation of a resolution inflammation phase (Fig. 4 *F and G* and *SI Appendix*, Fig. S4I). On the other hand, pooled serum multiplex analysis of circulating cytokine showed that control diet-fed $Cmah^{-/-}Ldlr^{-/-}$ mice had some baseline increases (*SI Appendix*, Fig. S4M) but HFD attenuated the differences with the exception of inflammatory cytokines such as interleukin (IL)-5 and IL-12p 70 (*SI Appendix*, Fig. S4N).

Overall the increased inflammation in $Cmah^{-/-}Ldlr^{-/-}$ mice was more pronounced in the atherosclerotic lesions (Fig. 4G), meaning that greater local, rather than systemic, inflammation is the more prominent driver of increased atherosclerosis in the *Cmah*-null mice.

The Combination of Human-Like Anti–Neu5Gc Antibodies and Neu5Gc–HFD Further Increases Atherogenesis in $Cmah^{-/-}Ldlr^{-/-}$ Mice. Due to the lack of Neu5Gc production most humans develop circulating anti-Neu5Gc antibodies (42, 43). Unlike humans, $Cmah^{-/-}Ldlr^{-/-}$ mice do not spontaneously produce anti-Neu5Gc antibodies even after long-term feeding of Neu5Gc-rich chow (44). This is likely because human antibodies appear to be induced by exposure to commensal bacteria such as *Haemophilus influenzae*, which can take up trace amounts of free Neu5Gc originating from food sources and
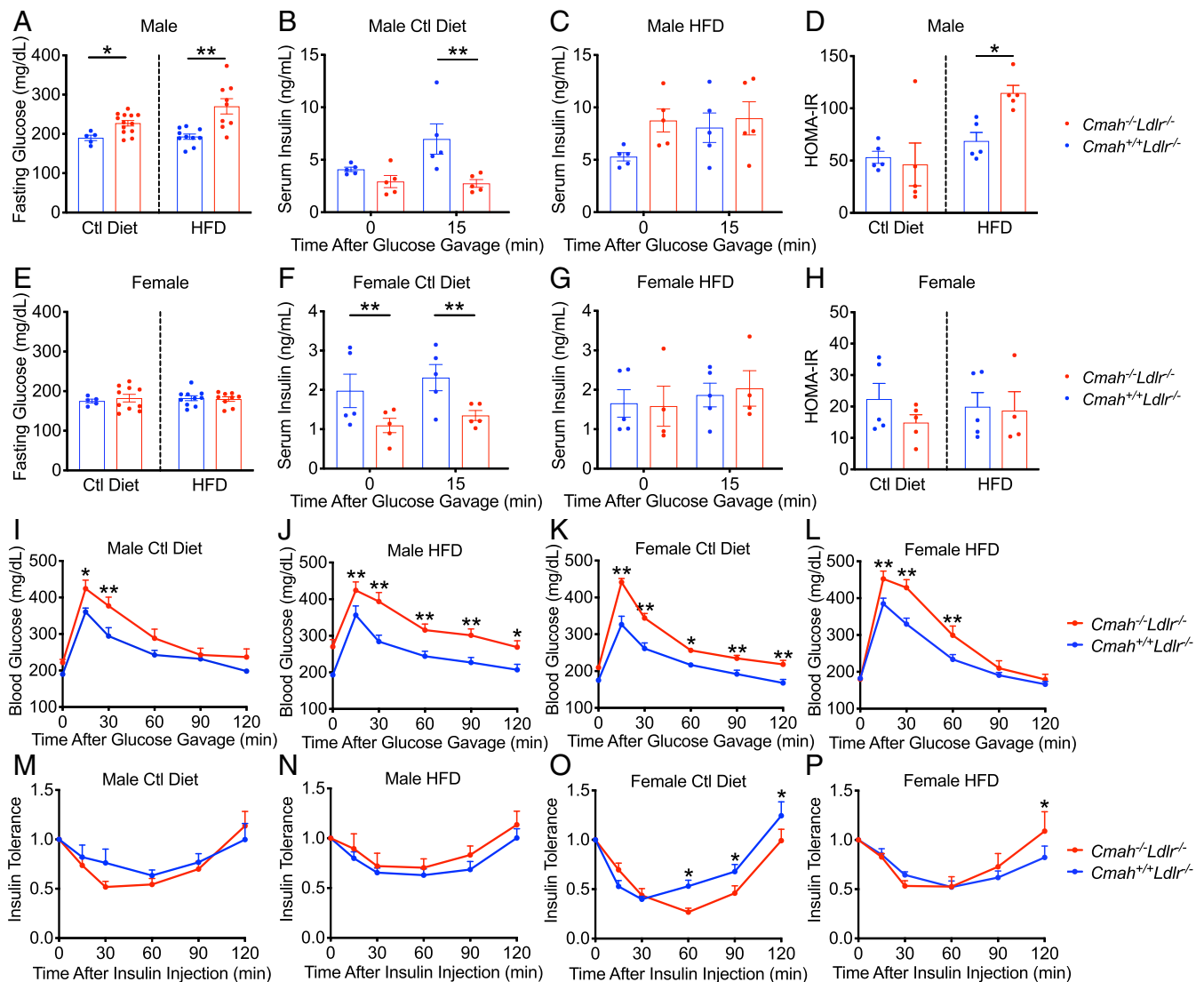
Fig. 3. Human-like $Cmah^{-/-}Ldlr^{-/-}$ mice have a hyperglycemic phenotype. $Cmah^{+/+}Ldlr^{-/-}$ and $Cmah^{-/-}Ldlr^{-/-}$ male and female mice were fed either a control diet or a HFD for 11 wk. (*A*) Fasting glucose level (male, $n = 5$ to 13), serum insulin levels before and 15 min after an oral glucose gavage in control diet (*B*) and HFD (*C*), and (*D*) homeostasis model assessment for insulin resistance (HOMA-IR) (male, $n = 5$ each). (*E*) Fasting glucose level (female, $n = 5$ to 10), serum insulin levels before and 15 min after an oral glucose gavage in control diet (*F*) and HFD (*G*), and (*H*) HOMA-IR (female, $n = 5$ each). (*I–L*) Glucose tolerance tests and (*M–P*) insulin tolerance tests (relative to basal glucose level) (male and female, $n = 10$ each). Mean values $\pm$ SEM, $*P < 0.05$ and $**P < 0.01$.

incorporate it into an immunogenic lipooligosaccharide (44). To study the extrinsic impact of CMAH loss we therefore immunized $Cmah^{-/-}Ldlr^{-/-}$ male mice with Neu5Gc-rich (Gc immunization) or control Neu5Ac-rich (Ctl immunization) red blood cell (RBC) ghosts (chimpanzee or human, respectively) in Freund's adjuvant before HFD feeding (Fig. 5*A*). One week after immunization, mice were put on HFD regimens with distinctly different compositions. To gauge the impact of Neu5Gc-feeding-induced xenosialitis on atherosclerosis development mice were put on a Neu5Gc-enriched HFD, with Neu5Ac-enriched and non-Sias HFD as controls. In the control immunization cohort, feeding a Neu5Gc-enriched HFD will not induce antibodies and xenosialitis, and as such controls for the impact of the dietary regimes and the immunization on atherogenesis independent of the Gc immunization.

The Neu5Gc-rich HFD regime in general did not induce major differences in body weight gain. Only mice on the Neu5Ac-rich diet seemed to have some decreased weight gain in the control immunization group (Fig. 5*B*) and increased weight gain with Gc immunization (Fig. 5*C*). There were no obvious

differences in plasma glucose levels, glucose tolerance, or insulin resistance between the different dietary groups (*SI Appendix*, Fig. S5 *A–D*). Interestingly, total cholesterol levels were significantly reduced in both Sias-rich HFD groups compared with the non-Sias HFD-fed mice both in the control immunization group (*SI Appendix*, Fig. S5*E*) and Gc immunization group (*SI Appendix*, Fig. S5*F*). The reduction in cholesterol levels was reflected by reduction in cholesterol content in the chylomicron/very-low-density lipoprotein fraction in the lipoprotein profile (*SI Appendix*, Fig. S5 *G* and *H*), but this was not as clear for the triglyceride distribution among lipoproteins (*SI Appendix*, Fig. S5 *I–L*).

A decrease in total cholesterol level would imply that Sias-rich feeding is atheroprotective. Despite this effect, the combination of Neu5Gc immunization and Neu5Gc-containing HFD actually aggravated atherosclerosis by 2.44-fold to 3.42-fold in the $Cmah^{-/-}Ldlr^{-/-}$ male mice as measured by *en face* analysis compared with the Neu5Ac-enriched HFD and the non-Sias HFD groups (Fig. 5 *D–F*). In the absence of Neu5Gc immunization
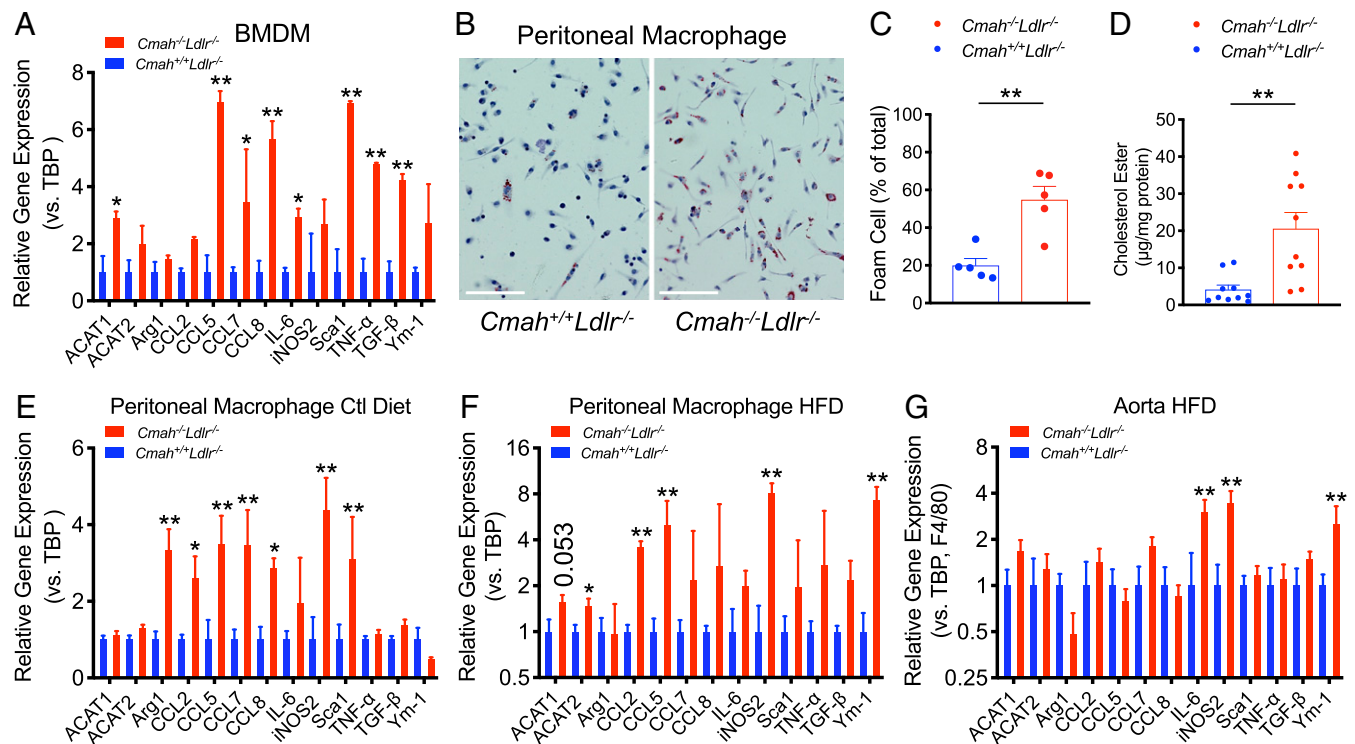
Fig. 4. Human-like $Cmah^{-/-}Ldlr^{-/-}$ macrophages show elevated inflammatory cytokine expression. (A) Cytokine gene expression in bone marrow-derived macrophages (BMDM) obtained from female mice, 8 to 12 wk age, that were fed with control chow ($n = 4$ each). (B) Oil red O staining of peritoneal macrophages collected from female after 12 wk of HFD. (Scale bars, 100 μm.) (C) Quantification of Oil red O-positive peritoneal macrophages (female, $n = 5$ each) and (D) cholesterol ester levels (female, $n = 10$ each). (E) Expression of inflammatory cytokines in peritoneal macrophages collected after 12 wk of feeding with either control chow or (F) HFD (female, $n = 8$ each). (G) Expression of inflammatory cytokines in atheroma lesions of aortic arch collected after 12 wk of HFD feeding (female, $n = 4$ each). Mean values ± SEM, *$P < 0.05$ and **$P < 0.01$.

the Neu5Gc-rich or Neu5Ac-rich HFD feeding did not affect atherosclerosis development in the aorta (Fig. 5 D and F). The Neu5Ac-enriched HFD also had no impact on atherosclerosis development in the aorta of Neu5Gc-immunized mice (Fig. 5 E and F).

Notably, the increased atherosclerotic surface area in the aortas was associated with a significant 3-fold increase in atherosclerotic lesion volume (Fig. 6 A–E) and a more advanced lesion phenotype characterized by an extensive 5-fold increase in necrotic core size (Fig. 6F). The increased atherogenesis in the xenosialitis model was not associated with dramatic differences in circulating inflammatory markers (haptoglobin and serum amyloid A; SI Appendix, Fig. S6 A and B) or by changes in plasma cytokines. IL-6 and IL-10 differed between groups but were not elevated xenosialitis group (Neu5Gc-immunized, Neu5Gc-rich HFD-fed) (SI Appendix, Fig. S6 C and D). Although some differences were observed in the inflammatory cell populations between the diet groups, those could not explain the increase atherogenesis in the Neu5Gc-immunized and Neu5Gc-rich HFD-fed male mice (SI Appendix, Fig. S6 E–L).

We confirmed that circulating anti-Neu5Gc antibodies were detected during HFD feeding regime in the Neu5Gc-immunized mice and absent in the control immunized cohorts (Fig. 6 G and H). We also confirmed Neu5Gc accumulation in the atheroma lesions (Fig. 6I and SI Appendix, Fig. S7), as we have previously shown in human samples (28). Human-like xenosialitis in atherosclerosis is confirmed in $Cmah^{-/-}Ldlr^{-/-}$ female mice as well (SI Appendix, Fig. S8B). However, the titer of anti-Neu5Gc antibody did not correlate with lesion size of atherosclerosis in the Neu5Gc-immunized Neu5Gc-HFD-fed group (in both male and female groups; SI Appendix, Fig. S8G). This is likely because the polyclonal antibody response is extremely complex and variable

between individuals, and no single epitope can be easily correlated with disease (43). In general, we show that the immune response to the metabolically incorporated foreign Neu5Gc in Gc-immunized $Cmah^{-/-}Ldlr^{-/-}$ mice fed a Neu5Gc-rich HFD was significantly correlated with the increased atherosclerosis development.

Discussion

The underlying question that drove this study was the common observation that humans appear to be particularly prone to cardiovascular complications of atherosclerosis, in comparison with other mammals. The question is whether this difference is purely due to the commonly known risk factors or whether genetic factors unique to human evolution also contribute. Here we present evidence to implicate the homozygous fixed state of CMAH inactivation as such an intrinsic factor, complicated by an extrinsic dietary factor that is also contingent on this mutation. We show first that human-like Cmah inactivation in mice enhances atherosclerosis via multiple intrinsic mechanisms. An additional CMAH mutation-dependent extrinsic factor is "xenosialitis," which arises from metabolic incorporation of the nonhuman sialic acid Neu5Gc (mimicking red meat intake) and polyclonal anti-Neu5Gc antibodies in the $Cmah^{-/-}Ldlr^{-/-}$ mouse model.

Given the plethora of cell types throughout the body affected by the loss of CMAH (20–24), it is not surprising that there is not one dominant pathway responsible for the marked increase in atherosclerosis development. In addition to higher immune activation, we did observe a strong diabetic phenotype in $Cmah^{-/-}Ldlr^{-/-}$ mice, which is a major driver of CVD in humans and to a lesser extent in mice. We have confirmed that glucose intolerance induced by HFD is more severe in $Cmah^{-/-}Ldlr^{-/-}$, without underlying insulin resistance, consistent with prior data (21).
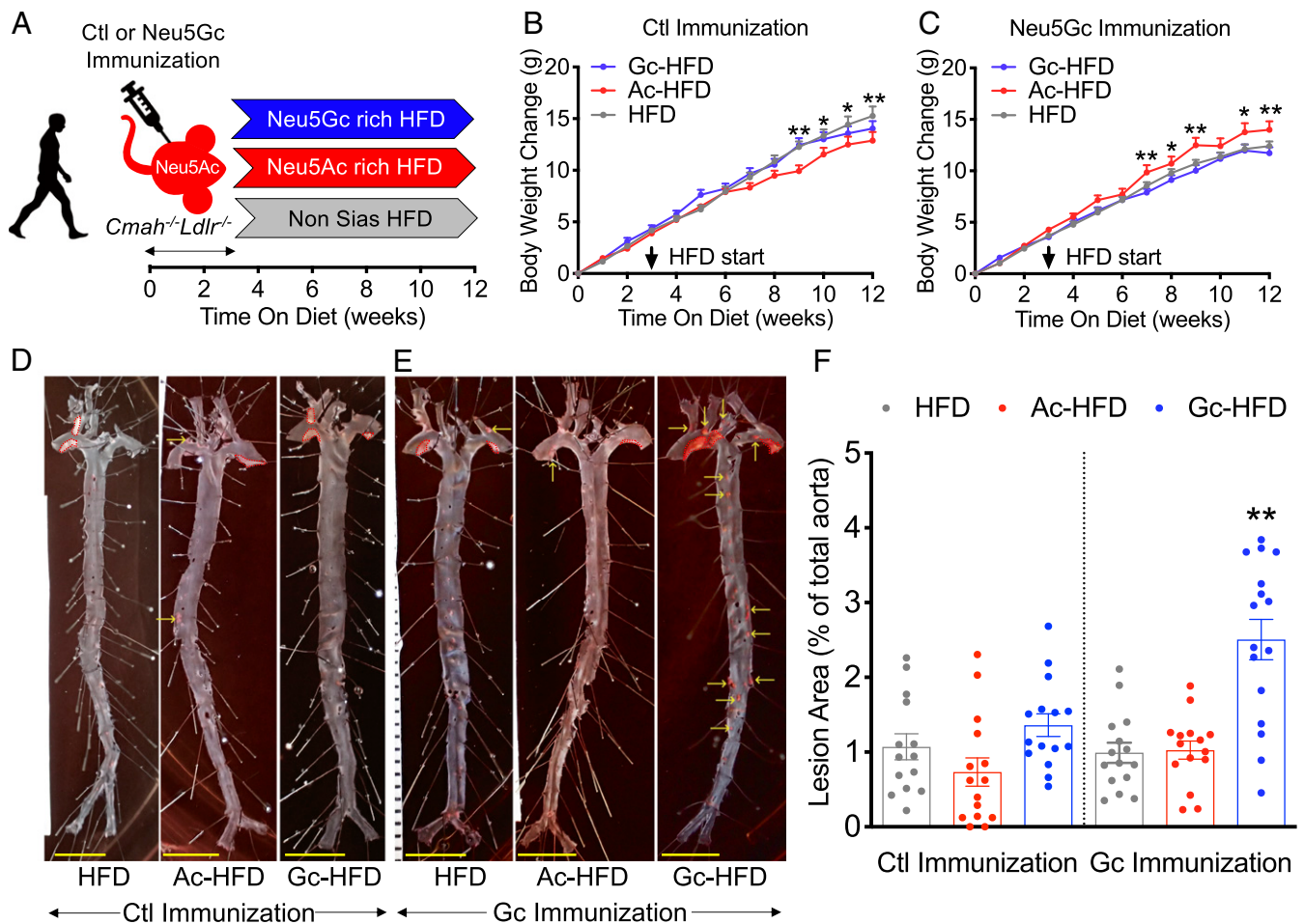
MEDICAL SCIENCES

Fig. 5. Combination of human-like anti-Neu5Gc antibodies and Neu5Gc-rich HFD increases atherogenesis. (*A*) *Cmah*⁻/⁻*Ldlr*⁻/⁻ male mice were immunized with either a control antigen (Ctl Immunization) or a Neu5Gc antigen (Gc Immunization) and then fed with a Neu5Ac-rich, Neu5Gc-rich, or non-Sias high-fat diet (Ac-HFD, Gc-HFD, and HFD, respectively) for 9 wk (*n* = 14 to 16, each). (*B* and *C*) Graphs representing body weight changes over 12 wk (HFD started at 9 wk of age, indicated by an arrow) in each group. *En face* analysis of atherosclerosis lesion (red dots and yellow arrows) in (*D*) control immunization and (*E*) Neu5Gc immunization groups. (Scale bars, 500 μm.) (*F*) Quantification of Sudan IV-positive area in aorta. Mean values ± SEM, *P* < 0.05 and **P* < 0.01.

According to the previous study, the diabetic phenotype in *Cmah*⁻/⁻ mice is explained by decreased islet size and numbers in pancreas (21) and the etiology is likely identical for our model. In our study, we measured inflammatory cytokine gene expression in pancreas; however, no significant difference was found between *Cmah*⁻/⁻*Ldlr*⁻/⁻ and *Cmah*⁺/⁺*Ldlr*⁻/⁻ (*SI Appendix*, Fig. S4*J*).

One factor we can exclude is that loss of *Cmah* expression affects cholesterol levels in the absence (or presence) of LDL receptor (LDLR) expression (45). In fact, circulating triglyceride, cholesterol, and LDL levels indicated by the lipoprotein profiles were unchanged between the groups in *Cmah*⁻/⁻*Ldlr*⁻/⁻ and *Cmah*⁺/⁺*Ldlr*⁻/⁻ mice fed with HFD and among *Cmah*⁻/⁻*Ldlr*⁻/⁻ mice, which were immunized with Neu5Gc or control antigen and a HFD containing either no Sias, Neu5Ac, or Neu5Gc. However, despite the lack of difference in circulating LDL-cholesterol levels, more foam cell conversion was observed in vivo in *Cmah*⁻/⁻*Ldlr*⁻/⁻ mice. It is known that increased inflammation can promote foam cell conversion and consequently drive atherosclerosis development (37–39). Indeed, this was observed in in *Cmah*⁻/⁻*Ldlr*⁻/⁻ mice with increased expression of ACAT1 and ACAT2, which can convert macrophages more efficiently into foam cells in the context of hypercholesterolemia. *Cmah*⁻/⁻ mouse macrophages showed stronger phagocytosis and cytokine production such as tumor necrosis factor-α and IL-6 than *Cmah*⁺/⁺ mouse macrophages, and similar differences

were seen in direct comparisons between human macrophage and chimp macrophages (22). Furthermore, Neu5Gc feeding of *Cmah*⁻/⁻ macrophages showed reduced phagocytosis in comparison Neu5Ac fed *Cmah*⁻/⁻ macrophages (22). There are also likely to be adaptive immune factors we did not pursue in this study. For example, *Cmah*⁻/⁻ mouse T cells showed a hyperactive phenotype following virus infection, and reintroduction of Neu5Gc to both human and *Cmah*⁻/⁻ T cells blunted their activation and proliferation during in vitro stimulation (23). *Cmah*-deficient mice also show a moderate B cell hyperactivity: The immune response to thymus-independent antigens was increased, calcium signaling after anti-immunoglobulin M stimulation was enhanced, and the marginal zone and recirculating B cell populations were decreased (24).

With regard to the extrinsic mechanism, the finding that only the combination of Neu5Gc antibodies and Neu5Gc-rich HFD feeding caused enhanced atherosclerosis indicates that the likely mechanism is antibody deposition with complement activation and/or recruitment of Fc receptor-positive leukocytes. However, these events probably occur early in the process, and we had difficulty showing clearly enhanced accumulation of antibody or complement in the extremely complex environment of the advanced atherosclerotic plaques, in which many other factors are operative. The obvious question arising from such experimental mouse studies is whether circulating anti-Neu5Gc antibodies
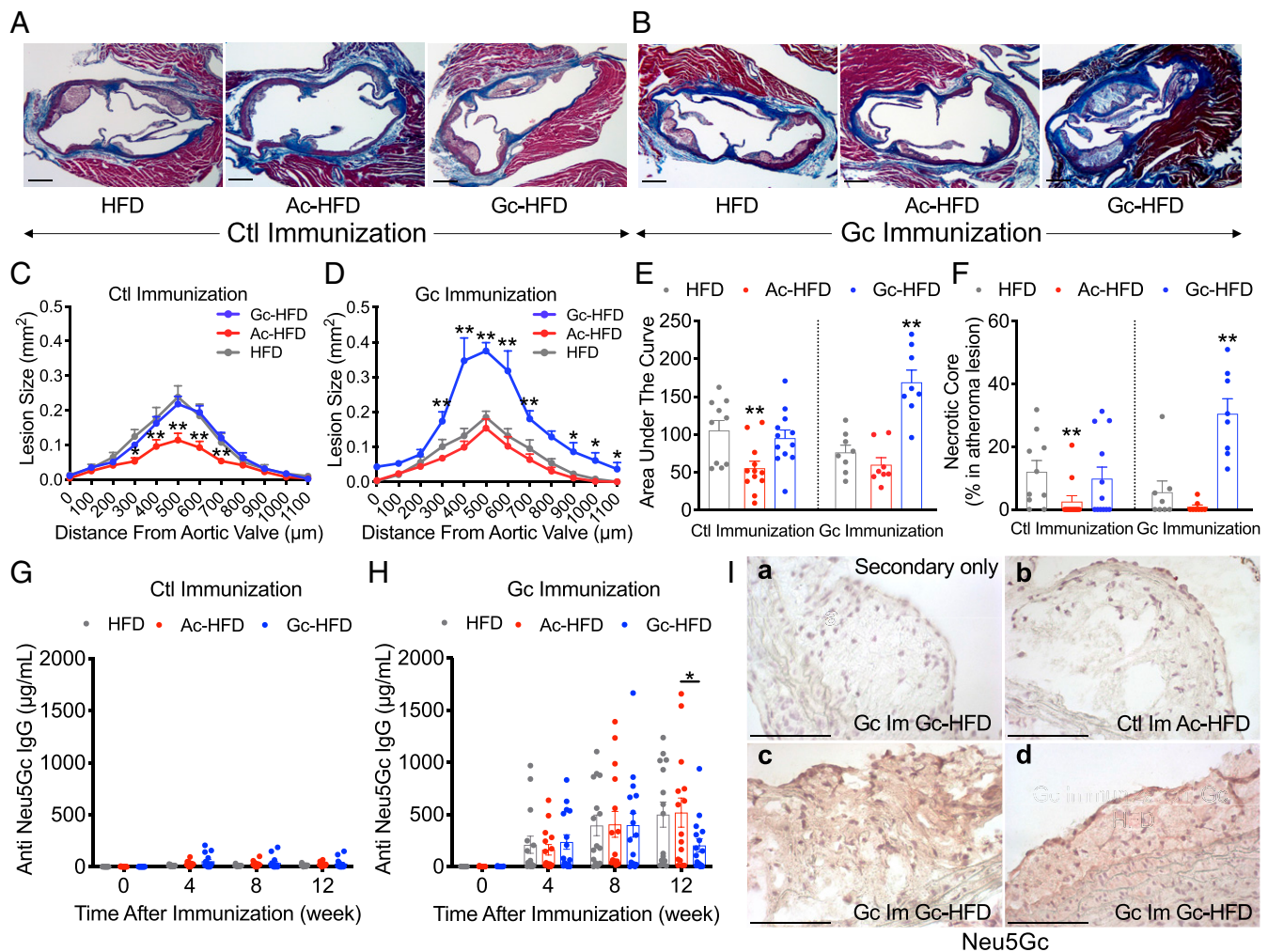
Fig. 6. Human-like anti-Neu5Gc antibodies and Neu5Gc-rich HFD induce advanced atheroma. $Cmah^{-/-}Ldlr^{-/-}$ male mice were immunized with either a control antigen (Ctl Immunization) or a Neu5Gc antigen (Gc Immunization) and then fed with a Neu5Ac-rich, Neu5Gc-rich, or non-Sias high-fat diet (Ac-HFD, Gc-HFD, and HFD, respectively) for 9 wk. (A and B) Atherosclerotic lesion in the aortic sinus. (C and D) Quantification of atherosclerotic lesion size in the aortic sinus. (E) Area under the curve. (F) Necrotic core size (male, $n = 8$ to 12). (G and H) Anti-Neu5Gc antibody titers measured by a bovine submaxillary mucin-coated ELISA (male, $n = 14$ to 16). (I) Representative images of expression of Neu5Gc in atheromas, using anti-Neu5Gc antibody immunohistochemistry: (a) secondary antibody (negative control) stain for Neu5Gc-immunized and Gc-HFD–fed mouse and Neu5Gc stains for (b) control immunized and Ac-HFD fed and (c and d) Neu5Gc-immunized and Gc-HFD–fed mice. (Scale bars, 100 μm.) Mean values ± SEM, *$P < 0.05$ and **$P < 0.01$.

correlate with CVD risk in human population studies. We are currently exploring this possibility (43) but are also aware of the numerous complicating variables in humans, such as the varying amount and unknown bioavailability of Neu5Gc from dietary red meat, the amount of Neu5Gc loading in tissues, the complex and variable polyclonal antibody profiles of individual humans, the skewed distribution of antibody levels within populations, and the variability of concurrent inflammatory conditions (30). Also, given that CMAH deletion results in variable loss of a major cell-surface molecule (Neu5Gc) and a corresponding increase in the precursor Neu5Ac throughout the body, it is not surprising that there is no single dominant mechanistic explanation for the striking phenotypic changes found in this study; rather, there are multiple interactive mechanisms (Fig. 7).

Overall our work may help explain why atherosclerosis and resulting CVD complications are very common in humans and why these events rarely occur spontaneously in other mammals, in the absence of experimental or dietary manipulation. Future studies of atherosclerosis in mice may also benefit from using the more human-like $Cmah$-deficient background, in which lesion progression is greater. With regard to the xenosialitis phenom-

enon, further work is also necessary to determine the exact pathways by which Neu5Gc is taken up into tissues, and potential approaches to prevent or eliminate such incorporation are being explored. The current findings indicate that this unique example of inflammation driven by a metabolically incorporated dietary glycan (30) is pathologically relevant and may be involved in other inflammation-driven diseases that are known to be associated with red meat consumption, including carcinomas (25), which also appear to be rare in chimpanzees (46).

Methods

Ethics Statement. The proposed use of mice in this project was approved by the University of California San Diego (UCSD) Animal Subjects Committee (Evaluation of the Role of Glycans in Normal Physiology, Malignancies and Immune Responses, Protocol S01227). All procedures were approved by the Animal Care Program and Institutional Animal Care and Use Committee, UCSD. Human RBCs and LDL were obtained from venous blood provided by healthy volunteers with informed consent under a protocol approved by UCSD Human Research Protection Programs Institutional Review Board.

Mice and Cell Culture. $Cmah^{-/-}Ldlr^{-/-}$ mice were generated by crossing $Cmah^{-/-}$ mice (47) and $Ldlr^{-/-}$ mice (48) in a congenic C57BL/6 background
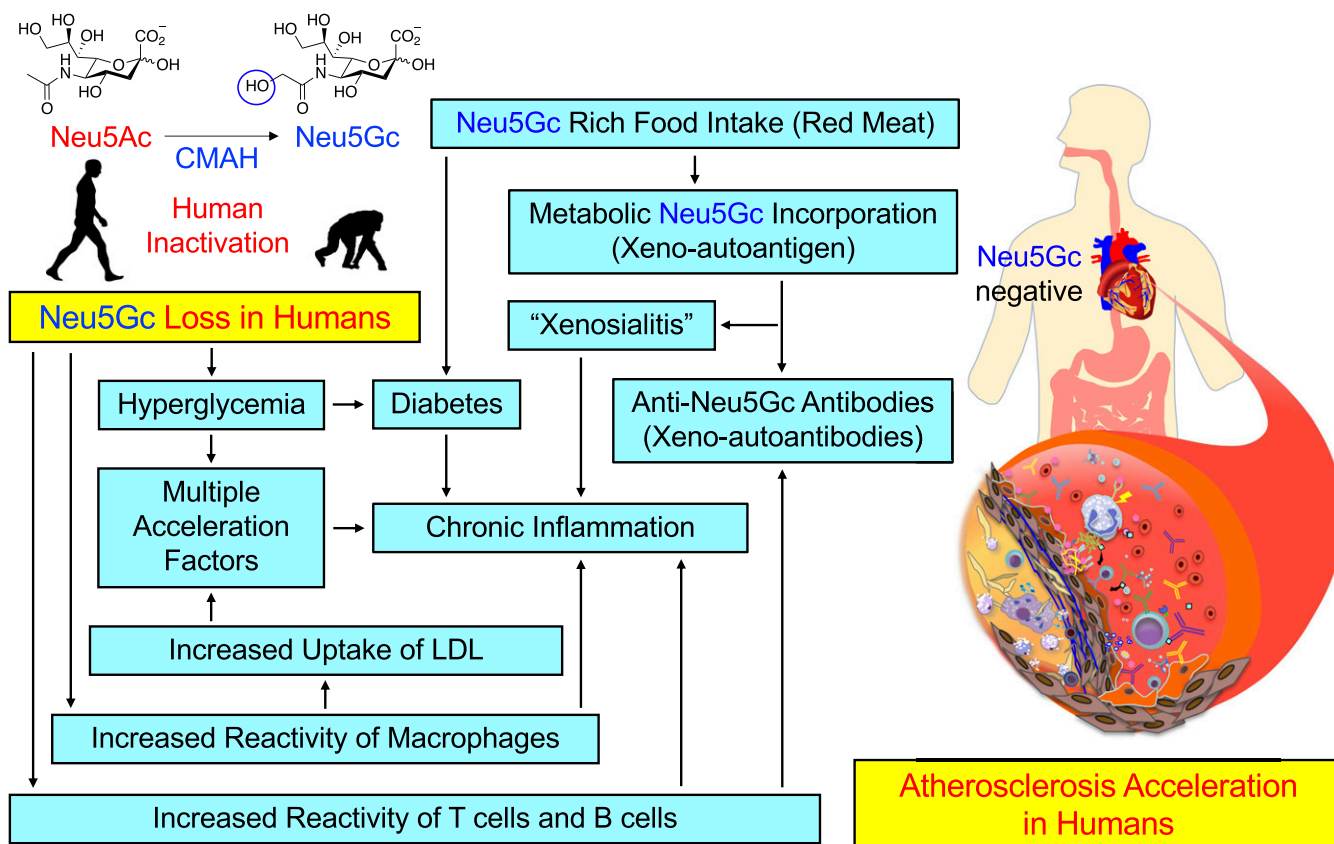
Fig. 7. Human species-specific loss of Neu5Gc increases atherosclerosis risk by multiple mechanisms. Inactivation of the CMP-*N*-acetylneuraminic acid (Neu5Ac) hydroxylase (CMAH) occurred ~2 to 3 Mya in the hominin lineage, which is now manifest as a human species-specific deficiency of the common mammalian sialic acid *N*-glycolylneuraminic acid (Neu5Gc). This Neu5Gc loss contributes to atherosclerosis risk via intrinsic mechanisms such as up-regulated inflammatory response and hyperglycemia as well as extrinsic mechanisms such as red meat-derived Neu5Gc-induced xenosialitis.

and maintained in the UCSD vivarium according to Institutional Review Board guidelines for the care and use of laboratory animals. All animals were fully back-crossed and maintained on a 12-h light cycle and fed water and standard rodent chow for ad libitum consumption. $Cmah^{-/-}Ldlr^{-/-}$ and $Cmah^{+/+}Ldlr^{-/-}$ mice were also maintained on a control soy-based (Sias-free) chow after weaning at 3 wk. At 6 or 9 wk of age male and female mice were placed on a Sias-free soy-based HFD with 20% anhydrous milkfat and 0.2% cholesterol, a Neu5Gc-rich soy-based HFD containing 0.25 mg of Neu5Gc per gram of chow and made by adding purified porcine submaxillary mucin (PSM) as described previously (29), or a Neu5Ac-rich soy-based HFD containing 0.25 mg of Neu5Ac per gram of chow, made by adding edible bird's nest (EBN) (Golden Nest, Inc.) (29). The amount of Neu5Gc in PSM and Neu5Ac in EBN was determined by HPLC with Neu5Ac (Nacalai) and Neu5Gc (Inalco) standards at UCSD and all chows were subsequently formulated and composed (Dyets, Inc.). Peritoneal macrophages were collected by peritoneal lavage after 12 wk of control diet or HFD feeding without any stimulants, and BMDMs were isolated from 8- to 12-wk-old female mice as described previously (37). BMDMs were maintained in M-CSF (Tonbo Biosciences) culture with lipoprotein-free bovine serum (Alfa Aesar) then fed with normal human LDL, ag LDL (40), or ox LDL (41). Macrophages or foam cell numbers were counted in a microscope and cholesterol ester level were measured with a kit (Invitrogen) and normalized with protein concentration (Thermo Fisher Scientific).

Neu5Gc and Control Immunization. Chimpanzee and human RBC membrane ghosts were prepared as described previously (29). Six-week-old $Cmah^{-/-}Ldlr^{-/-}$ male and female mice were immunized three times per week via intraperitoneal (i.p.) injection with pooled RBC membrane chimp ghosts (chimp, Neu5Gc 151.5 pmol/μg protein, Neu5Ac 24.1 pmol/μg protein, measured by HPLC) or control human ghosts (human, Neu5Gc 0.0 pmol/μg protein, Neu5Ac 97.7 pmol/μg protein, measured by HPLC), mixed with an equal volume of Freund's adjuvant.

Serum Lipoprotein and Lipid Analysis. Blood samples were obtained by mandibular plexus bleeding and cardiac puncture from mice fasted for 5 h. Plasma lipoproteins in 100-μL pooled samples were separated by size-exclusion chromatography using a polyethylene filter column (Sigma-Aldrich). Liver samples were homogenized in 250 mM sucrose buffer and the protein levels were measured by the bicinchoninic acid assay (Thermo Fisher Scientific). Cholesterol and triglyceride levels in separated lipoprotein fraction were measured by enzymatic kits (Sekisui) as well as total cholesterol and triglyceride levels in plasma and liver samples.

Glucose Tolerance and Insulin Tolerance Test and HOMA-IR. Mice received an oral glucose gavage (2 mg/g body weight) for glucose tolerance test or an i.p. injection of recombinant human insulin (Novo Nordisk) for insulin tolerance test (0.5 U/kg body weight) after 5 h of fasting. Blood glucose levels were measured using blood collected via tail vein bleeding just before and at 15, 30, 60, 90, and 120 min after oral glucose or injection of insulin with the Accu-Chek Aviva glucose monitoring system (Roche Applied Science GmbH). Insulin levels were measured with the ultrasensitive mouse insulin ELISA kit (Chrystal Chem). HOMA-IR was calculated as follows:

$$HOMA\text{-}IR = 26 \times \text{fasting insulin level (ng / mL)}$$
$$\times \text{ fasting glucose level(mg / dL) / 405.}$$

Quantification of Aortic Atherosclerosis. Mice were killed by isoflurane intoxication and perfused with a PBS–10% neutral buffered formalin solution. The heart and ascending aorta down to the iliac bifurcation were dissected using stereomicroscopy, the aortas were dissected open along the long axis, pinned flat and stained for lipids using Sudan IV. Serial 10-μm cryosections of the aortic sinus were stained with Masson's trichrome to measure total atherosclerosis lesion, collagen fiber lesion, and necrotic core lesion area. Each parameter was calculated using ImageJ blindly by K.K. and R.D.

Quantification of Inflammatory Cytokine Gene Expression. Cells or organs were collected after completion feeding regimen and mRNA was collected using a purification kit and converted into cDNA (Qiagen, Inc.). Expression of each cytokine gene (*SI Appendix*, Table S1) was measured using Cyber Green systems (Qiagen, Inc.).

Immunohistochemistry. All aorta tissue samples were either flash frozen in OCT or fixed and processed for paraffin sections, and were stained with H&E, Masson-Trichrome, Oil Red O, Terminal TUNEL was done using an In Situ Cell Death Detection Kit (TMR red) as per kit manufacturer's (Roche) instructions and counterstained with Hoechst (ThermoFisher), or with immunohisto-chemistry using anti-F4/80 (Bio-Rad/AbD Serotec), anti-CD68 (Abcam), and anti-Neu5Gc (BioLegend) counterstained with Mayer's hematoxylin, on se-rial cross sections of the aortic sinus. TUNEL positive cells in aortic sinus and Oil Red O lipid positive areas in liver samples were photographed using Keyence BZ-X800 (KEYENCE, Cop.). Each parameter was measured using Image J and Keyence BZ-X800 blindly by K.K., C.D., and R.D.

Blood Cell Analysis and Quantification of Serum Inflammatory Cytokine. Whole EDTA blood samples were analyzed in duplicate for complete blood count with differential leukocyte count were performed with a Hemavet 850FS Multi Species Hematology System (Drew Scientific) in mouse hematology settings. Serum haptoglobin (Life Diagnostics, Inc.) and serum amyloid pro-tein A (Life Diagnostics, Inc.) were measured according to the manufacturers' instructions. Multiplex inflammatory cytokine levels were measured with proinflammatory panel 1 (mouse) kits (Meso Scale Diagnostics, LLC).

ELISA Detection of Anti-Neu5Gc Antibodies in Mice Serum. Microtiter plate wells were coated with Neu5Gc-rich bovine submaxillary mucin (Sigma) in sodium carbonate-bicarbonate buffer at 4 °C overnight. Wells were in-cubated with 1:100 dilutions of mouse serum at room temperature for 2 h. Thereafter, wells were incubated with HRP-conjugated goat anti-mouse IgG. Mild periodate treatment is used to selectively cleave sialic acid side-chains and eliminate specific reactivity, as described previously (29).

Statistical Analysis. All data were analyzed by Student's *t* test, Mann–Whitney *U* test, Kruskal–Wallis test, 1-way ANOVA, or 2-way ANOVA, Pearson correlation coefficient and presented as mean ± SEM. Statistical analyses were performed using Prism software (version 8; GraphPad Software). *P* values less than 0.05 were considered significant.

1. I. Tabas, G. García-Cardeña, G. K. Owens, Recent insights into the cellular biology of atherosclerosis. *J. Cell Biol.* **209**, 13–22 (2015).
2. J. G. Canto *et al.*; NRMI Investigators, Number of coronary heart disease risk factors and mortality in patients with first myocardial infarction. *JAMA* **306**, 2120–2127 (2011).
3. T. Robinson *et al.*, New Zealand Diabetes Cohort Study cardiovascular risk score for people with Type 2 diabetes: Validation in the PREDICT cohort. *J. Prim. Health Care* **4**, 181–188 (2012).
4. D. Denton *et al.*, The effect of increased salt intake on blood pressure of chimpanzees. *Nat. Med.* **1**, 1009–1016 (1995).
5. N. Varki *et al.*, Heart disease is common in humans and chimpanzees, but is caused by different pathological processes. *Evol. Appl.* **2**, 101–112 (2009).
6. T. Huby *et al.*, Functional analysis of the chimpanzee and human apo(a) promoter sequences: Identification of sequence variations responsible for elevated transcrip-tional activity in chimpanzee. *J. Biol. Chem.* **276**, 22209–22214 (2001).
7. H. Laurence *et al.*, Natural mortality and cause of death analysis of the captive chimpanzee (Pan troglodytes): A 35-year review. *J. Med. Primatol.* **46**, 106–115 (2017).
8. L. J. Lowenstine, A primer of primate pathology: Lesions and nonlesions. *Toxicol. Pathol.* **31** (suppl.), 92–102 (2003).
9. L. J. Lowenstine, R. McManamon, K. A. Terio, Comparative pathology of aging great apes: Bonobos, chimpanzees, gorillas, and orangutans. *Vet. Pathol.* **53**, 250–276 (2016).
10. N. M. Varki, E. Strobert, E. J. Dick , Jr, K. Benirschke, A. Varki, Biomedical differences between human and nonhuman hominids: Potential roles for uniquely human as-pects of sialic acid biology. *Annu. Rev. Pathol.* **6**, 365–393 (2011).
11. M. L. Lammey, D. R. Lee, J. J. Ely, M. M. Sleeper, Sudden cardiac death in 13 captive chimpanzees (Pan troglodytes). *J. Med. Primatol.* **37** (suppl. 1), 39–43 (2008).
12. S. B. Eaton, M. Konner, M. Shostak, Stone agers in the fast lane: Chronic degenerative diseases in evolutionary perspective. *Am. J. Med.* **84**, 739–749 (1988).
13. J. H. J. O'Keefe , Jr, L. Cordain, Cardiovascular disease resulting from a diet and lifestyle at odds with our Paleolithic genome: How to become a 21st-century hunter-gatherer. *Mayo Clin. Proc.* **79**, 101–108 (2004).
14. M. D. Gurven *et al.*, Cardiovascular disease and type 2 diabetes in evolutionary per-spective: A critical role for helminths? *Evol. Med. Public Health*, eow028 (2016).
15. R. C. Thompson *et al.*, Atherosclerosis across 4000 years of human history: The Horus study of four ancient populations. *Lancet* **381**, 1211–1222 (2013).
16. E. M. Clarke *et al.*, Is atherosclerosis fundamental to human aging? Lessons from ancient mummies. *J. Cardiol.* **63**, 329–334 (2014).
17. A. N. Gabrovsky, K. D. O'Neill, E. Gerszten, Paleopathology of cardiovascular diseases in South American mummies. *Int. J. Cardiol.* **223**, 101–107 (2016).
18. H. H. Chou *et al.*, A mutation in human CMP-sialic acid hydroxylase occurred after the Homo-Pan divergence. *Proc. Natl. Acad. Sci. U.S.A.* **95**, 11751–11756 (1998).
19. T. Hayakawa, I. Aki, A. Varki, Y. Satta, N. Takahata, Fixation of the human-specific CMP-N-acetylneuraminic acid hydroxylase pseudogene and implications of haplotype diversity for human evolution. *Genetics* **172**, 1139–1146 (2006).
20. J. Okerblom, A. Varki, Biochemical, cellular, physiological, and pathological consequences of human loss of N-glycolylneuraminic acid. *ChemBioChem* **18**, 1155–1171 (2017).
21. S. Kavaler *et al.*, Pancreatic beta-cell failure in obese mice with human-like CMP-Neu5Ac hydroxylase deficiency. *FASEB J.* **25**, 1887–1893 (2011).
22. J. J. Okerblom *et al.*, Loss of CMAH during human evolution primed the monocyte-macrophage lineage toward a more inflammatory and phagocytic state. *J. Immunol.* **198**, 2366–2373 (2017).
23. G. Buchlis *et al.*, Enhanced T cell function in a mouse model of human glycosylation. *J. Immunol.* **191**, 228–237 (2013).
24. Y. Naito *et al.*, Germinal center marker GL7 probes activation-dependent repression of N-glycolylneuraminic acid, a sialic acid species involved in the negative modulation of B-cell activation. *Mol. Cell. Biol.* **27**, 3008–3022 (2007).
25. F. Alisson-Silva, K. Kawanishi, A. Varki, Human risk of diseases associated with red meat intake: Analysis of current theories and proposed role for metabolic in-corporation of a non-human sialic acid. *Mol. Aspects Med.* **51**, 16–30 (2016).
26. M. Bardor, D. H. Nguyen, S. Diaz, A. Varki, Mechanism of uptake and incorporation of the non-human sialic acid N-glycolylneuraminic acid into human cells. *J. Biol. Chem.* **280**, 4228–4237 (2005).
27. P. Tangvoranuntakul *et al.*, Human uptake and incorporation of an immunogenic nonhuman dietary sialic acid. *Proc. Natl. Acad. Sci. U.S.A.* **100**, 12045–12050 (2003).
28. T. Pham *et al.*, Evidence for a novel human-specific xeno-auto-antibody response against vascular endothelium. *Blood* **114**, 5225–5235 (2009).
29. A. N. Samraj *et al.*, A red meat-derived glycan promotes inflammation and cancer progression. *Proc. Natl. Acad. Sci. U.S.A.* **112**, 542–547 (2015).
30. C. Dhar, A. Sasmal, A. Varki, From "serum sickness" to "xenosialitis": Past, present, and future significance of the non-human sialic acid Neu5Gc. *Front. Immunol.* **10**, 807 (2019).
31. Z. Wang *et al.*, Gut flora metabolism of phosphatidylcholine promotes cardiovascular disease. *Nature* **472**, 57–63 (2011).
32. R. A. Koeth *et al.*, Intestinal microbiota metabolism of L-carnitine, a nutrient in red meat, promotes atherosclerosis. *Nat. Med.* **19**, 576–585 (2013).
33. W. H. Tang *et al.*, Intestinal microbial metabolism of phosphatidylcholine and car-diovascular risk. *N. Engl. J. Med.* **368**, 1575–1584 (2013).
34. B. J. Bennett *et al.*, Trimethylamine-N-oxide, a metabolite associated with atheroscle-rosis, exhibits complex genetic and dietary regulation. *Cell Metab.* **17**, 49–60 (2013).
35. E. Nagy *et al.*, Red cells, hemoglobin, heme, iron, and atherogenesis. *Arterioscler. Thromb. Vasc. Biol.* **30**, 1347–1353 (2010).
36. D. J. Schaer, P. W. Buehler, A. I. Alayash, J. D. Belcher, G. M. Vercellotti, Hemolysis and free hemoglobin revisited: Exploring hemoglobin and hemin scavengers as a novel class of therapeutic proteins. *Blood* **121**, 1276–1284 (2013).
37. P. L. S. M. Gordts *et al.*, Reducing macrophage proteoglycan sulfation increases ath-erosclerosis and obesity through enhanced type I interferon signaling. *Cell Metab.* **20**, 813–826 (2014).
38. I. Tabas, A. H. Lichtman, Monocyte-macrophages and T cells in atherosclerosis. *Im-munity* **47**, 621–634 (2017).
39. M. E. Kotas, R. Medzhitov, Homeostasis, inflammation, and disease susceptibility. *Cell* **160**, 816–827 (2015).
40. J. S. Frank, A. M. Fogelman, Ultrastructure of the intima in WHHL and cholesterol-fed rabbit aortas prepared by ultra-rapid freezing and freeze-etching. *J. Lipid Res.* **30**, 967–978 (1989).
41. J. L. Witztum, A. H. Lichtman, The influence of innate and adaptive immune re-sponses on atherosclerosis. *Annu. Rev. Pathol.* **9**, 73–102 (2014).
42. V. Padler-Karavani *et al.*, Cross-comparison of protein recognition of sialic acid di-versity on two novel sialoglycan microarrays. *J. Biol. Chem.* **287**, 22593–22608 (2012).
43. A. N. Samraj *et al.*, Polyclonal human antibodies against glycans bearing red meat-derived non-human sialic acid N-glycolylneuraminic acid are stable, reproducible, complex and vary between individuals: Total antibody levels are associated with co-lorectal cancer risk. *PLoS One* **13**, e0197464 (2018).
44. R. E. Taylor *et al.*, Novel mechanism for the generation of human xeno-autoantibodies against the nonhuman sialic acid N-glycolylneuraminic acid. *J. Exp. Med.* **207**, 1637–1646 (2010).
45. J. D. Horton, J. C. Cohen, H. H. Hobbs, Molecular biology of PCSK9: Its role in LDL metabolism. *Trends Biochem. Sci.* **32**, 71–77 (2007).
46. N. M. Varki, A. Varki, On the apparent rarity of epithelial cancers in captive chim-panzees. *Philos. Trans. R. Soc. Lond. B Biol. Sci.* **370**, 20140225 (2015).
47. M. Hedlund *et al.*, N-glycolylneuraminic acid deficiency in mice: Implications for hu-man biology and evolution. *Mol. Cell. Biol.* **27**, 4340–4346 (2007).
48. S. Ishibashi *et al.*, Hypercholesterolemia in low density lipoprotein receptor knockout mice and its reversal by adenovirus-mediated gene delivery. *J. Clin. Invest.* **92**, 883–893 (1993).